

## Metallicity-dependent Spectral Evolution

Peeter Traat

*Tartu Observatory, EE2400 Tartu, Estonia*

### 1. Introduction

The initial chemical composition of stars is, besides the mass, another key factor in stellar evolution. Through stellar lifetimes and impact on radiation output and nucleosynthesis of stars it is controlling both the pace of evolution of galactic matter/light and changes in their integrated observables and spectra.

This aspect of galactic evolution has been for a long time ignored in quantitative studies, because the real breakthrough in availability of sets of homogeneous non-solar composition stellar evolutionary tracks and atmospheres occurred only in the last few years. Presently there exist two consistent track sets with sufficient range of metallicities - set for 5 compositions produced by the Geneva group (cf. Meynet et al. 1994, with earlier references therein; lately a sixth, high-metallicity  $Z = 0.10$  composition got added to the set by Mowlavi et al. 1998) and the Padova tracks (cf. Girardi et al. 1996, and references therein), the latter covering with 8 compositions practically all the observable and theoretically useful metallicity interval from  $Z = 0.0001$  to  $Z = 0.10$ . Both still pose some further problems for applications(ors) - the Geneva tracks do not include for non-solar compositions post-RGB stages of evolution of low-mass stars  $M \leq 1.7 M_{\odot}$ , so these have to be added from other (and inhomogeneous) sources, plus they cover a shorter range in abundances. The Padova tracks are relatively free of such basic problems, except for a lack of stars  $M > 9 M_{\odot}$  in the  $Z = 0.10$  subset, but some minor irregularities arise also for the  $Z = 0.001$  composition because they were computed with different radiative opacities. As to the coupling of  $Z$ -dependent chemical evolution with spectrophotometry, the Geneva tracks have had the advantage of having stellar nucleosynthetic results available from the onset (Maeder 1992), although for just two compositions,  $Z = 0.001$  and  $Z = 0.02$ . That gap of missing yields for the Padova set finally got filled by a recent publication of Portinari et al. (1998), for the first time putting the future combined chemo-spectro-photometric models on a firm footing.

### 2. Discussion of spectral data

We have used both track sets to study the spectral evolution of stellar populations as functions of their initial metallicity and star formation parameters. No gas emission/dust absorption has been considered in these models, since it is highly individual for galaxies. On the basis of Padova tracks and isochrones we have some time ago released a standardized grid of spectral data files (Traat 1996), computed with the evolutionary codes developed by the author. The

Table 1. Time-integrated energy fluxes of coeval stellar populations with different IMF slopes and metallicities, per 1  $M_{\odot}$  in massive stars 10 to 120  $M_{\odot}$ . Flux units  $10^{52}$  erg, flux fractions  $f_i$  computed for intervals 90.9-395 Å, 395-995 Å, 995-1995 Å, 1995-3590 Å, 3590-7490 Å, 0.749-4.99  $\mu\text{m}$  and 4.99-160  $\mu\text{m}$ .

n	Z	L	$f_1$	$f_2$	$f_3$	$f_4$	$f_5$	$f_6$	$f_7$
1.0	0.001	0.2944	.0792	.2585	.4691	.1090	.0635	.0206	.0002
	0.004	0.2977	.0503	.2429	.4932	.1153	.0695	.0284	.0002
	0.008	0.2896	.0383	.2465	.5128	.1170	.0590	.0262	.0003
	0.020	0.2629	.0243	.2408	.5265	.1172	.0539	.0368	.0005
	0.040	0.2305	.0096	.2012	.5476	.1367	.0659	.0385	.0005
1.6	0.001	0.3169	.0579	.2025	.4809	.1239	.0911	.0434	.0004
	0.004	0.3147	.0365	.1902	.4896	.1263	.0988	.0579	.0006
	0.008	0.3074	.0271	.1880	.5032	.1287	.0919	.0603	.0007
	0.020	0.2824	.0166	.1799	.5020	.1256	.0888	.0859	.0012
	0.040	0.2487	.0067	.1527	.5175	.1412	.0962	.0844	.0012
2.0	0.001	0.3897	.0376	.1405	.4561	.1388	.1393	.0868	.0009
	0.004	0.3746	.0239	.1339	.4546	.1365	.1444	.1055	.0012
	0.008	0.3678	.0174	.1296	.4578	.1375	.1420	.1144	.0014
	0.020	0.3458	.0103	.1201	.4352	.1291	.1419	.1611	.0023
	0.040	0.2997	.0043	.1052	.4519	.1415	.1441	.1509	.0021
2.2	0.001	0.4691	.0274	.1064	.4253	.1459	.1741	.1197	.0013
	0.004	0.4399	.0176	.1027	.4200	.1411	.1772	.1397	.0016
	0.008	0.4337	.0127	.0982	.4162	.1403	.1775	.1533	.0019
	0.020	0.4159	.0073	.0888	.3811	.1278	.1778	.2141	.0030
	0.040	0.3538	.0032	.0799	.4000	.1388	.1782	.1973	.0027
2.35	0.001	0.5620	.0205	.0823	.3947	.1502	.2029	.1477	.0016
	0.004	0.5159	.0133	.0805	.3872	.1436	.2049	.1684	.0019
	0.008	0.5106	.0095	.0762	.3779	.1411	.2070	.1861	.0023
	0.020	0.4985	.0053	.0674	.3346	.1249	.2063	.2578	.0037
	0.040	0.4166	.0024	.0621	.3547	.1350	.2066	.2359	.0032
2.5	0.001	0.6974	.0148	.0613	.3599	.1532	.2319	.1769	.0020
	0.004	0.6256	.0097	.0607	.3505	.1452	.2336	.1980	.0023
	0.008	0.6221	.0068	.0568	.3360	.1405	.2372	.2201	.0027
	0.020	0.6198	.0037	.0490	.2864	.1204	.2340	.3021	.0043
	0.040	0.5075	.0017	.0464	.3071	.1298	.2355	.2757	.0037
2.7	0.001	0.9767	.0090	.0391	.3115	.1551	.2681	.2148	.0024
	0.004	0.8492	.0060	.0394	.2997	.1458	.2706	.2358	.0027
	0.008	0.8506	.0041	.0363	.2793	.1377	.2754	.2640	.0032
	0.020	0.8719	.0022	.0303	.2255	.1126	.2666	.3577	.0050
	0.040	0.6937	.0010	.0297	.2451	.1211	.2717	.3270	.0044
3.0	0.001	1.7551	.0038	.0183	.2447	.1540	.3122	.2641	.0030
	0.004	1.4602	.0026	.0188	.2295	.1437	.3183	.2839	.0032
	0.008	1.4817	.0017	.0169	.2035	.1306	.3229	.3206	.0038
	0.020	1.5820	.0009	.0133	.1510	.0993	.3025	.4269	.0060
	0.040	1.2094	.0004	.0138	.1660	.1063	.3152	.3931	.0052
3.4	0.001	4.2012	.0011	.0060	.1768	.1485	.3510	.3130	.0036
	0.004	3.3257	.0007	.0063	.1585	.1382	.3636	.3290	.0037
	0.008	3.4400	.0005	.0054	.1303	.1191	.3651	.3752	.0044
	0.020	3.8395	.0002	.0040	.0867	.0828	.3286	.4907	.0069
	0.040	2.8204	.0001	.0044	.0948	.0875	.3505	.4567	.0060
4.0	0.001	16.8714	.0002	.0010	.1147	.1383	.3811	.3604	.0043
	0.004	12.6020	.0001	.0011	.0950	.1293	.4026	.3678	.0041
	0.008	13.4144	.0001	.0009	.0693	.1037	.3968	.4243	.0050
	0.020	15.6599	.0000	.0006	.0396	.0647	.3416	.5457	.0078
	0.040	11.1299	.0000	.0007	.0415	.0662	.3711	.5137	.0067

grid includes 1008 models and has the widest practically useful range of chemical compositions and star formation prescriptions. It covers all the Padova set abundance range, i.e. eight metallicities  $Z = 0.0001, 0.0004, 0.001, 0.004, 0.008, 0.02, 0.05$  and  $0.10$ . The conversion from stellar luminosities and temperatures to spectral flux distributions was based on Kurucz (1993) model atmospheres with the prospect of their future replacement in the cool star region,  $T_{eff} \leq 4500$  K, from a new Uppsala release.

The dataset for each  $Z$  value includes

- six power law IMFs of different slopes  $1.6 - 3.5$ ,
- corresponding single-generation populations
- populations with continuous/continuing star formation for those IMFs with 4 SFR index values  $s = 0$  (constant SFR),  $s = 1$  (exponentially declining),  $s = 1.5$  and  $2$  (initially faster, later slower than the exponential SFR) and 5 star-formation timescales  $0.2, 1, 2, 5$  and  $15$  Gyr.

Spectra are presented for 50 ages in the case of starburst populations and 20 ages for populations with continuous star formation. Ages range from  $0.003$  Gyr to  $20$  Gyr.

The models are chemically homogeneous, no nebular component/absorption has been included. SFR has been parametrized by a power of the gas volume density (as introduced by Schmidt (1959)), with index  $s$  and time-scale  $t_0$ . In this context, the single-generation (“initial-burst”) populations with their independency on the SFR/its power index form the limiting “starburst”  $t_0 = 0$  case.

Metallicity growth affects the stellar evolution in two ways: first, making stars cooler and dimmer, secondly, redistributing their flux through opacity growth at short wavelengths towards longer wavelengths. So the total result of a  $Z$  increase on the composite spectrum of a stellar population is the progressive erosion of flux in ultraviolet region, and the faster, the shorter the wavelength. However, with the enhancement of absorption in metallic lines in the UV, the bulk of energy reradiated in the optical and near-infrared is increasing with the definite net result that the spectrum level at  $\lambda \geq 1 \mu\text{m}$  is for all population ages progressively higher for higher metallicities.

Table 1 gives a general quantitative review of the extent of metallicity effects in different spectral regions for populations with different mass function slopes  $n$ . Time is eliminated by integration over the lifetimes of stars, population mass is scaled to the unit amount of mass in very massive stars  $M \geq 10 M_{\odot}$ . The Geneva set of tracks (5 compositions, the latest  $Z = 0.10$  subset was not included yet) was used. These data testify, that composition-caused flux changes can be rather impressive, extending to a factor of 10 in the far-UV and  $\sim 2$  in infrared.

To illustrate metallicity effects graphically, we also provide a couple of examples on Fig. 1, computed with Padova tracks. On the left panel of this figure we have plotted computed spectra of coevally formed stellar populations (so-called *initial burst* populations) with 8 different initial metallicities  $Z$ , having ages  $1$  Gyr. Such comparatively blue spectra are typical for medium-aged star clusters of assumed chemical compositions, or young elliptical galaxies with ages somewhat exceeding  $1$  Gyr. The flux of models is scaled to the unit mass in luminous stars with masses  $M > 0.6 M_{\odot}$ , the IMF in these graphs is a power-law with slope  $n = -2.35$  (“Salpeter” value). The most metal-deficient,  $Z = 0.0001$

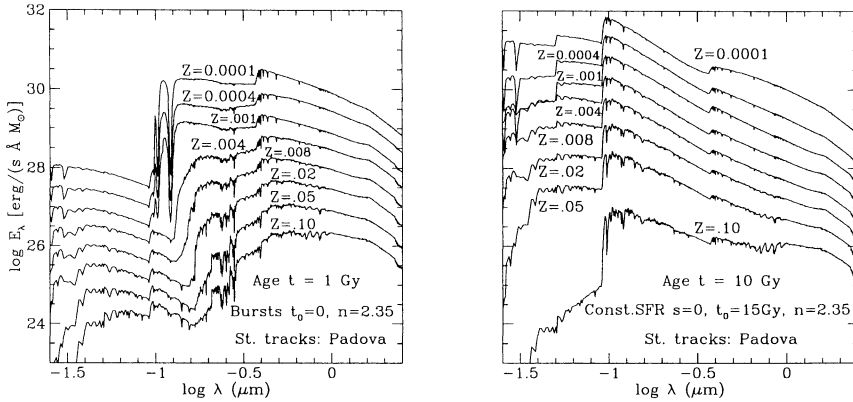


Figure 1. Composition dependence of spectra of stellar populations: coevally formed young stellar populations (age 1 Gyr, *left panel*) and old populations with constant SFR (age 10 Gyr, *right panel*).

spectrum has a correct location in  $\log E_\lambda$ , all the others have been successively shifted downwards by additional 0.5 dex, with maximum total shift  $-3.5$  for the  $Z = 0.10$  case. On the right panel the spectra of old, 10 Gyr stellar populations, are plotted, in which star formation is continuous and proceeds with a constant, time-independent intensity over the eon  $t_0$ . This case might be considered as a kind of approximation to late spirals or irregulars, since in many of these the actual SFRs do not seem to significantly differ from the mean average over their past. Notice, however, that due to the actively continuing star formation the ultraviolet flux of models keeps sizable. The growth of metal content sharply reduces the flux at shorter wavelengths, as also on the left-panel plot.

**Acknowledgements.** I would like to express my gratitude to the LOC of Symposium and Tartu Cultural Capital for support, facilitating my participation in the meeting.

## References

- Meynet, G., Maeder, A., Schaller, G., Schaerer, D., Charbonnel, C. 1994, *A&AS*, 103, 97
- Girardi, L., Bressan, A., Chiosi, C., Bertelli, G., Nasi, E. 1996, *A&AS*, 117, 113
- Kurucz, R. 1993, *ATLAS9 Stellar Atmosphere Programs and 2 km/s grid* (Kurucz CD-ROM No. 13)
- Maeder, A. 1992, *A&A*, 264, 105
- Mowlavi, N., Schaerer, D., Meynet, G., Bernasconi, P.A., Charbonnel, C., Maeder, A. 1998, *A&AS*, 128, 471
- Portinari, L., Chiosi, C., Bressan, A. 1998, *A&AS*, 304, 505
- Schmidt, M. 1959, *ApJ*, 129, 243
- Traat, P. 1996, *AAS*, CD-ROM vol. 7.